AD_____

GRANT NUMBER DAMD17-97-1-7325

TITLE: Development of Guidelines for the Prophylactic Treatment of Metastatically Involved Vertebral Bodies

PRINCIPAL INVESTIGATOR: Cari M. Whyne

CONTRACTING ORGANIZATION: University of California, San Francisco
San Francisco, California 94143-0962

REPORT DATE: August 1998

TYPE OF REPORT: Annual

PREPARED FOR: Commanding General
U.S. Army Medical Research and Materiel Command
Fort Detrick, Maryland 21702-5012

REPORT DOCUMENTATION PAGE

Form Approved
OMB No. 0704-0188

1. AGENCY USE ONLY *(Leave blank)*	2. REPORT DATE	3. REPORT TYPE AND DATES COVERED
	August 1998	Annual (15 Jul 97 - 14 Jul 98)

4. TITLE AND SUBTITLE
Development of Guidelines for the Prophylactic Treatment of Metastatically Involved Vertebral Bodies

5. FUNDING NUMBERS
DAMD17-97-1-7325

6. AUTHOR(S)
Cari M. Whyne

7. PERFORMING ORGANIZATION NAME(S) AND ADDRESS(ES)
University of California, San Francisco
San Francisco, California 94143-0962

8. PERFORMING ORGANIZATION REPORT NUMBER

9. SPONSORING / MONITORING AGENCY NAME(S) AND ADDRESS(ES)
U.S. Army Medical Research and Materiel Command
Fort Detrick, Maryland 21702-5012

10. SPONSORING / MONITORING AGENCY REPORT NUMBER

11. SUPPLEMENTARY NOTES

12a. DISTRIBUTION / AVAILABILITY STATEMENT
Approved for Public Release; Distribution Unlimited

12b. DISTRIBUTION CODE

19990219106

13. ABSTRACT *(Maximum 200 words)*

Up to 1/3 of all cancer patients develop metastases to the spinal column and over 50% of spinal metastases with neurologic manifestations in females are found to arise from primary breast neoplasms (3). Burst fracture can arise in such bones compromised by tumor and is deemed one of the most difficult injuries of the spine to treat successfully, in part because the exact injury mechanism is not well understood. Using a combination of finite element modeling, materials and mechanical testing we aim to quantify fracture risk in metastatically involved vertebral bodies in order to both understand the mechanism of such fractures and develop a definitive set of clinical guidelines for the prophylactic treatment vertebral body metastases. To this end, we have developed an experimental protocol to analyze biphasic material properties of tumor specimens. We have constructed a poroelastic two-dimensional axis-symmetric finite element model of the vertebral body and adjacent intervertebral disc which has enabled us to parametrically assess the effects of rate dependence on vertebral body strength and validate the importance of utilizing poroelastic theory in the consideration of metastatic involvement. This progress provides us the needed basis for our three-dimensional modeling and experimental validation necessary to quantify burst fracture risk.

14. SUBJECT TERMS	15. NUMBER OF PAGES
Breast Cancer	22
	16. PRICE CODE

17. SECURITY CLASSIFICATION OF REPORT	18. SECURITY CLASSIFICATION OF THIS PAGE	19. SECURITY CLASSIFICATION OF ABSTRACT	20. LIMITATION OF ABSTRACT
Unclassified	Unclassified	Unclassified	Unlimited

FOREWORD

Opinions, interpretations, conclusions and recommendations are those of the author and are not necessarily endorsed by the U.S. Army.

____ Where copyrighted material is quoted, permission has been obtained to use such material.

____ Where material from documents designated for limited distribution is quoted, permission has been obtained to use the material.

____ Citations of commercial organizations and trade names in this report do not constitute an official Department of Army endorsement or approval of the products or services of these organizations.

____ In conducting research using animals, the investigator(s) adhered to the "Guide for the Care and Use of Laboratory Animals," prepared by the Committee on Care and use of Laboratory Animals of the Institute of Laboratory Resources, national Research Council (NIH Publication No. 86-23, Revised 1985).

CW For the protection of human subjects, the investigator(s) adhered to policies of applicable Federal Law 45 CFR 46.

____ In conducting research utilizing recombinant DNA technology, the investigator(s) adhered to current guidelines promulgated by the National Institutes of Health.

____ In the conduct of research utilizing recombinant DNA, the investigator(s) adhered to the NIH Guidelines for Research Involving Recombinant DNA Molecules.

____ In the conduct of research involving hazardous organisms, the investigator(s) adhered to the CDC-NIH Guide for Biosafety in Microbiological and Biomedical Laboratories.

Lori Wynne Aug 5, 98

PI - Signature Date

TABLE OF CONTENTS

INTRODUCTION

Breast, prostate, lung and renal cancers are the most common primary tumors which metastasize to bone. The vertebral column is the most frequent skeletal site for metastases (29) and due to the proximity to the spinal cord, 5% to 10% of all cancer patients develop neurologic manifestations (3). Up to 1/3 of all cancer patients develop metastases to the spinal column and over 50% of spinal metastases with neurologic manifestations in females are found to arise from primary breast neoplasms (3). For instance, in a 15 month study conducted by Toma et al. (28) 74.5% of patients with malignant tumors and secondary bone involvement had a primary tumor located in the breast, of which 54.5% had secondary spinal involvement. Unfortunately, there is no established method for assessing the prognosis of patients with breast cancer and metastasis confined initially to bone (30), yet bone metastases are a major source of morbidity in patients with breast cancer (13). In the face of greater life expectancy for women with breast cancer, spinal metastases are an increasing source of morbidity which negatively affects patients' long term quality of life.

Yearly there are about 18,000 new cases of metastatic involvement of the vertebral body in the United States, often resulting in vertebral instability (1). Metastases to the spinal column may be detected by radiographs, bone scan or may present with symptoms of pain, paralysis, loss of sensation or bowel and bladder control. Fracture risk prediction has significant clinical importance, as prevention of fracture in high risk patients may be possible through medical prophylaxis, use of external bracing, or internal stabilization. While the majority of vertebral body fractures occur anteriorly, posterior body (burst) fractures can arise from high impact loading or normal loading in bones compromised by osteoporosis or tumor. Burst fracture is one of the most difficult injuries of the spine to successfully treat, in part because the exact mechanism by which the distraction forces are transmitted to the intracanal fragments of the burst fracture have not been adequately investigated (8). The average survival time of breast cancer patients with vertebral involvement is 99.4 months, or 40.4 months from the time of diagnosis of the bone metastases (2). Longer survival times for patients with metastatic disease, especially from primary breast tumors, have increased the incidence of pathologic fracture.

While improved imaging modalities allow clinicians to better determine the extent of bony metastases, assessing the risk of neurologic compromise is guesswork at best. In a review of 70 cases of spinal cord compression in breast cancer, Hill et al. (9) found that all patients had radiologic evidence of bone metastases at the time of spinal cord compression. The majority of their patients had warning symptoms of spinal cord compression and nearly all had evidence of vertebral metastases before compression occurred. Accurate neurologic risk assessment would benefit patients by providing more aggressive treatment options. Clinical and radiographic studies have concluded that early and aggressive treatment of vertebral body metastases should be considered to improve patients' life quality (9,28). Elective stabilization with posterior instrumentation and fusion in high risk patients is preferable to emergent decompression and uncertain neurologic recovery. In patients with burst fractures resulting in spinal cord or cauda equina compression, complete recovery following surgical intervention occurs in only 1/3 of patients (26). Although neurologic recovery was better in younger female patients suffering from metastatic breast cancer than in older men with prostatic metastases (26), prevention of vertebral body fracture and spinal cord compression would considerably reduce the morbidity arising from vertebral body metastases. Especially in cases of long life expectancy with tumors like breast cancer, posterior decompression and stabilization can exert a long-term therapeutic effect (22). A

better understanding of spinal canal risk may permit some patients to avoid surgery altogether, an important goal in patients with limited life expectancy.

Investigations have looked at the relative contributions to load sharing as well as age related changes and other pathologic processes affecting the spine, yet most have focused on anterior failures rather than posterior body (burst) fracture patterns. Previous methods used for strength assessment in the vertebral body have included finite element modeling, computed tomography and in vitro mechanical testing (6,12,16,18,23,24,27). The non-invasive techniques can be employed to provide clinical information on the location and magnitudes of defects and stresses in bones and for prediction of fracture risk (10,17). Determination of vertebral body strength can provide information on the risk of vertebral body failure including fracture location and potential for canal encroachment. Previous work has identified metastatic breast cancer lesions at risk of fracture in the femur with retrospective clinical record and radiographic examination (15) and for lesions in the femoral neck with finite element analysis validated through mechanical testing (5).

Previous studies have attempted to predict fracture risk of metastatically involved vertebral bodies using defects modeled as voids, neglecting any effects from the mass and fluid behaviour of tumor material (6,19,20,25). Mizrahi et al. (20) developed a finite element model to study the effects of metastatic lesions on the vertebral body strength. The study used a symmetric model and represented the defects simply as voids. They found, not surprisingly, that larger defects, particularly when involving greater than 40% of the vertebra, were likely to result in greater risk of fracture in the anterior-superior part of the vertebral body. The study, however, did not address the effects these defects have on creating a potential risk of burst fracture and associated canal compromise.

An in vitro experimental study of metastatic lesions in the thoracic vertebrae was performed by McGowan et al. (19) to predict that strength reductions were associated with a reduction in vertebral cross sectional area. Mechanical testing of vertebral bodies with experimentally produced trabecular bone defects was performed under axial-flexion loads. The results suggested that strength reduction due to lytic defects, considered as voids within the thoracic vertebrae, is proportional to the cross sectional area of the removed bone. However, in no case was the posterior vertebral body wall found to be displaced into the canal after failure. Similar mechanical testing was performed in vitro by Silva et al. (25). They found significantly lower failure loads for vertebrae with lesions regardless of the position of the defect. However all failures occurred in the anterior vertebral body without damage of the posterior wall, thus again the true effect of the defects on posterior stability and the risk of neurologic deficit was not addressed. Dimar et al. (6) also recently tested spinal motion segments containing defects drilled as a cylinder through the trabecular centrum as well as the anterior and posterior cortical walls. This removal of posterior cortex eliminates the possibility of assessing the risk of posterior fracture or neurologic compromise.

In Mizrahi's finite element model and the mechanical testing of McGowan et al., Silva et al. and Dimar et al., the defects were modeled as voids, neglecting any effects which may arise due to the mass and fluid behaviour of tumor material. Clinically, encroachment of either tumor material or displaced bone may result in canal compromise, thus the mass effect of the tumor is likely to be significant. Consequently, although these studies give some insight into the type of lesion which may put a patient at risk for compression fracture, they do not consider which lesions pose a risk for neurologic deficit.

The mechanism of burst fracture has been clinically suggested to be due to entry of the nucleus of the disc into the vertebral body through an endplate fracture causing the body to pressurize and ultimately burst (11), thus indicating poroelastic behaviour (the rate dependent behaviour of a tissue containing both a solid and a fluid phase) .The two phase porous behaviour of trabecular bone has been demonstrated by Carter and Hayes (4) through confined compression testing of bone with and without marrow. The presence of marrow increased the strength, modulus and energy absorption of the specimens when tested at a strain rate which would simulate loading conditions found in high energy burst fractures. Downey et al. (7) found an increase in intraosseus pressure in an intact bone structure under compressive loading. Shirado et al. (23) tested vertebral body motion segments (vertebra-disc-vertebra) under axial compression and were able to reproduce such burst fracture patterns. These studies examined solid specimens of trabecular bone and vertebral bodies devoid of any defects. In metastatically involved vertebral bodies however the tumor mass consists of a solid matrix with greatly reduced elastic stiffness and a large percentage of fluid. This large fluid mass may cause the effect of loading rate on bone fracture to be more pronounced. In vertebral bodies compromised by tumor, burst fracture patterns are found to occur under physiologic loading conditions similar to that which occur in healthy vertebrae only under high energy impact. Yet an analysis of the poroelasticity of trabecular bone within intact vertebral bodies, with or without metastatic involvement, has not been studied. Nor have any studies on metastatically involved vertebral bodies included the two phase nature of the tumor. If metastatically involved vertebral bodies exhibit poroelastic behaviour under physiologic loading rates, fracture prediction estimates from earlier models may not accurately represent the stress distributions in the vertebral body.

Guidelines are needed to permit clinicians to select appropriate patients for intervention before the development of neurologic compromise. Current guidelines for prophylactic stabilization have been extrapolated from clinical experience and subjective intuition rather than from experimental evidence. Suggested indications for stabilization include: >50% vertebral body destruction, pedicle destruction, involvement of two or more adjacent vertebral bodies, involvement of anterior and posterior elements, progressive collapse of a vertebral body, and severe pain not relieved by other treatments. A widely accepted definitive set of guidelines for prophylactic intervention in metastatically involved vertebral bodies has yet to be determined.

The purpose of our research is to quantify fracture risk in vertebral bodies affected by metastatic breast cancer in order to develop a set of clinical guidelines for the prophylactic treatment of patients with such metastases. We hypothesize that the use of poroelastic theory in modeling will yield more realistic estimates of fracture prediction compared to values based on a linear elastic model and that poroelastic properties of both bone and tumor tissue are necessary to understand the mechanisms of vertebral body failure and adequately assess the risk of neurologic compromise. The ultimate goal of this research is to use engineering analysis to develop clinical diagnostic and surgical guidelines for prophylactic stabilization of metastatically involved vertebral bodies in order to prevent paralysis and significantly improve the quality of life of patients with vertebral body metastases.

In our initial proposal during the first year we planned to determine the poroelastic properties of breast tumor tissue and develop both a two dimensional axisymmetric and a three dimensional metastatically involved vertebral body model. The following is a summary of our progress towards those goals.

BODY

Technical Objective 1: Poroelastic properties of tumor tissue

To determine the poroelastic properties of breast tumor tissue. Tissue properties will be measured experimentally through confined compression testing of human tumor specimens obtained at surgery from bone metastases.

To establish the mechanical properties of the metastatic tumor material in terms of linear poroelastic theory we have set up creep experiments on tumor specimens in confined compression (Figure 1). The outcome variables for each specimen are the aggregate compressive modulus (H_A) and the hydraulic permeability (k). Tumor tissue will be harvested at surgery from patients with metastatic involvement of bone, and frozen. Cylindrical test specimens (1-2 mm thick x 5 mm diameter) are prepared by first cutting out blocks of 1-2 mm thickness using a vibratome, and then punching out the 5 mm diameter plugs directly into the confining chamber (Figure 2).

Specimens inside the cylindrical confining chamber are sandwiched between rigid, porous glass platens. Normal saline is added to the chamber and the compressive creep tests performed in the bath held at body temperature (37° C). A constant load of 0.4 to 1 g is applied to the specimen to achieve a final strain of <20%. Tests are conducted until equilibrium is achieved (1 to 24 hours). Due to possible inaccuracies in the load application through the counterweighted arm, an additional load cell is included to record the actual force felt by the specimen. The creep displacement versus time data is filtered and collected using LABVIEW 5.0 and fit to a solution derived using linear poroelastic theory (necessitating the small strain requirements of the experimental protocol). The parameters H_A and k are determined using non-linear best-fit regression (MATLAB, v5.0). Based on clinical availability thus far, eight tumor samples have been collected from a variety of tumor metastases to bone. Although acquiring a sufficient number of specimens for the study has taken longer than expected, we do not anticipate this to be a limitation in the final project. The histology of each tumor is analyzed to determine the cellular content and percentage of necrosis. Results of stiffness and permeability will ultimately be correlated with these parameters to discover whether such parameters (available from biopsy) can be reliable indicators of tumor tissue material properties.

Difficulties in the execution of the testing protocol have occurred due to the very small loads needed to maintain the small strain conditions necessary to implement linear poroelastic theory. Initially a confined compression testing set up was designed using an MTS. However, it became evident that the feedback control on such a large machine was not adequate to maintain constant loads at these small magnitudes. As such, our experimental apparatus was designed and built to apply constant load without the necessity of a variable feedback loop. Further difficulties have resulted due to friction between the specimen or platens and the confining chamber. Due to the small applied loads, overcoming such frictional forces can prove troublesome

The results and subsequent curve fit to determine the material parameters H_A and k from one specimen of metastatic breast tumor tissue are shown in Figure 3. While only a very limited number of specimens have been tested, thus far the aggregate moduli of the tumor tissue tested have been within the range of 0.001 to 0.005 MPa. This includes both specimens from primary

lung and breast neoplasms. However, the hydraulic permeability of the specimens thus far differ by several orders of magnitude from values in the range of 10^{-1} to 10^{-3}. This may ultimately be explained by the difference in histology of the specimens. The results from the breast metastasis tested in Figure 3 had a hydraulic permeability on the order of 10^{-1} and consisted of a highly cellular tissue (up to 75% in some areas) with large areas of necrosis. In contrast, one lung specimen tested demonstrated a hydraulic permeability on the order of 10^{-3} and was made up of a considerable amount of stroma with a cellularity of approximately 30% and less than 10% necrosis. More analyses and specimens are needed before and conclusions can be drawn about the material properties of tumor tissue which has metastasized to bone.

Technical Objective 2: Poroelastic theory applied to metastatically involved vertebral body modeling

To develop a poroelastic two-dimensional axis-symmetric finite element model of the vertebral body and parametrically assess the effects of rate dependence on vertebral body strength and the implications of poroelastic theory in the consideration of metastatic involvement in the model.

We developed a two-dimensional poroelastic axisymmetric finite element model of a spinal motion segment consisting of the first lumbar vertebral body and adjacent intervertebral disc (Figure 4). The model assumed a midsagittal axis of symmetry and a transverse plane of symmetry. No posterior elements were modeled. A finite element mesh consisting of 493 elements (8-noded quads and rebars) was generated and analyzed using commercial software (PATRAN 5.0, ABAQUS 5.6). The model was constructed to allow the inclusion of a centrally located tumor in the vertebral body, representing a 25% or 50% defect of the trabecular bone by volume. An elastic model with the number of elements increased by a factor of four was generated and demonstrated mesh convergence was reached in the initial model.

The intact model (no tumor included) was analyzed under a fully elastic configuration (both disc and vertebral body represented with elastic material properties), with a poroelastic disc attached to a linear elastic vertebral body (with and without restricted flow through the cartilaginous endplate), and as a fully poroelastic model. In the analyses of the metastatically involved cases only poroelastic modeling was performed.

The vertebral body was composed of a cortical shell and endplate modeled isotropically and a transversely isotropic trabecular bone centrum, with properties (both elastic and poroelastic) chosen to represent a healthy young spine (14). The intervertebral disc consisted of cartilaginous endplate, nucleus pulposus and annulus fibrosus. The nucleus and cartilaginous endplate were modeled isotropically in the elastic and poroelastic configurations. The annulus was composed of an isotropic material modeled hyperelastically in both configurations and reinforced with rebar elements representing collagen fibers. The tumor tissue was modeled as a poroelastic isotropic material with the aggregate modulus and hydraulic permeability varied to represent a spectrum of material properties found in lytic lesions. In the poroelastic and mixed analyses, the fluid phase for all tissues was modeled as incompressible with properties equivalent to water.

The model was loaded axially under a uniform pressure of 1 MPa applied though the midplane of the intervertebral disc (which corresponds to a 1200N force, approximating the compressive force on the lumbar spine for an individual standing upright holding an 8.3 kg mass

with outstretched arms (21)). The intact poroelastic model was analyzed under a range of loading rates from 10,000 MPa/s (impact) to 4 MPa/s (slow walking). In the mixed elastic/poroelastic runs a physiologic loading rate level of 100MPa/s was applied. In the analyses of the metastatically involved cases poroelastic modeling was performed under loading rates of 10 MPa/s and 100MPa/s.

We focused on trabecular bone failure and our outcome variables were: radial displacement of the vertebral body midline (U1) as an indicator for spinal canal encroachment, endplate deformation (U2) as a measure of endplate fracture, maximum strain (E) indicating potential trabecular bone failure, and pore pressure (POR) to determine the amount of load carried by the fluid phase in the poroelastic analyses.

When we represented the vertebral body elastically, our results were dependent on the disc representation used (elastic versus poroelastic) (Table 1). Greater disc deformation in the axial and radial directions in the fully elastic model create different loading conditions applied to the cortical endplate of the vertebral body, and thus yield significant differences in the trabecular bone outcome parameters (Figure 5). However, changes in the boundary conditions at the disc - vertebral body interface, from restricted flow to free flow through the endplate, did not result in significant differences in vertebral body response in the mixed models.

The fully poroelastic representation yielded higher maximum principal tensile strains and radial displacement and lower maximum principal compressive strains and axial displacement in the vertebral body trabecular bone than found in the mixed models. Conversely, results within the intervertebral disc under the fully poroelastic configuration are bounded by the results derived from the two mixed models.

Tumor size had the greatest effect on vertebral body displacement, strain and pore pressure in the poroelastic model (Table 2). Increasing tumor size from 25% to 50% yielded a 40% increase in maximum radial displacement, a 40% increase in tensile hoop and radial strains located at the axis of symmetry along the bone tumor interface, and a 130% increase in the compressive strain under the center of the endplate. Maximum trabecular bone displacement in the radial direction shifted from an area adjacent to the outer endplate in the intact vertebral body to the transverse midline when a defect was incorporated. Pore pressure in the vertebral body trabecular bone was increased by 160% and 280% respectively with the inclusion of 25% and 50% tumors into the vertebral body model as compared to the case with no tumor involvement (Figure 6).

In the intact poroelastic model, increase in loading rate resulted in a decrease in the maximum displacement in the radial direction at the distal edge of the model adjacent to the endplate, a site indicating a potential increased risk of compression fracture (Table 3). This was accompanied by an increase in the axial displacement under the endplate adjacent to the nucleus pulposus for loading rates up to 0.01 s^{-1}. This axial displacement was found to saturate under loading rates faster than 0.01 s^{-1}. As well, pore pressure within the vertebral body was found to decrease with increased loading rate in the intact model. Conversely, with a 10 fold reduction in loading rate in the pathologic models, maximum pore pressures in the vertebral body were reduced by 8% and demonstrated a smaller overall pore pressure gradient (Figure 4). This reduction in loading rate in the pathologic models also caused maximum endplate displacement and axial compressive strains to increase by 5% to 13%.

Variation of tumor tissue material properties did not have much influence on the model outcome parameters. A 10 fold increase in tumor tissue permeability was found to have no effect on our vertebral body results. However, a 25 fold increase in tumor aggregate modulus in the 50% defect model did result in small reductions in vertebral body strain (2% to 6%), displacement (0.5% to 3%) and pore pressure (2%).

In assessing the need for utilizing poroelastic modeling techniques in analyzing spinal motion segments, it was found that the boundary conditions applied to the vertebral body endplate are dependent on the constitutive assumptions of the intervertebral disc, and as such, affect the strain and displacement results in the trabecular bone centrum. Greater disc deformation in the axial and radial directions in the fully elastic model create different loading conditions applied to the cortical endplate of the vertebral body, and thus different responses within the vertebral body itself. For analyses aimed at studying the responses of the intervertebral disc alone, our results suggest it is reasonable to utilize a mixed model. That is, the results found in the intervertebral disc in the fully poroelastic model are bounded by the results derived from the mixed models; a free flow boundary at the endplate simulating a fully poroelastic model at a slow loading rate, and a no flow boundary condition simulating fast loading. However, results for strains and displacements in the poroelastic vertebral body are not bounded by the mixed model results. The inclusion of the fluid phase into the vertebral body results in a portion of the spinal load being supported by the liquid, reducing the solid strains in the axial direction in the trabecular bone. Concurrently, the incompressibility of the fluid phase causes expansion and higher strains to develop in the radial direction within the vertebral body.

In determining the effect of loading rate on a spinal motion segment it was found that as the loading rate was increased, higher values of compressive strains and lower values of tensile strains were predicted in the solid phase of the vertebral body trabecular bone. At the same time, maximum pore pressures within the nucleus were found to increase, while pore pressures in the vertebral body decreased. This opposing trend was due to the large disparity in the diffusion time constants of the nucleus (on the order of 10^5 s) versus the trabecular bone centrum (on the order of 10^{-1} s). As fluid does not have time to escape from the nucleus under higher loading rates, the incompressibility of the fluid phase in the nucleus causes increased axial deformation of the vertebral body endplate. These results agree with clinical observations indicating an increased likelihood for endplate failure in vertebral bodies loaded at higher rates, potentially leading to burst fracture patterns once the endplate fracture permits the nucleus to enter and pressurize the vertebral body.

In examining the relative effects of tumor size, material properties and loading rate in the assessment of metastatically involved vertebral bodies, increased tumor size was found to cause the greatest increase in vertebral body displacements, strains and pore pressure. The location of maximum displacement and pore pressures suggest a greater risk for endplate and radial vertebral body failure (i.e. an increased likelihood of vertebral burst fracture) as the size of defect increases. Greater maximum radial displacement values and increased tensile hoop strains predicted at the transverse midline of the vertebral body may potentially correspond to a catastrophic fracture pattern with bone and tumor encroachment into the spinal canal in a three-dimensional model. This finding agrees with the radiologic assessments of Taneichi *et al.* (Taneichi *et al.*, 1997), who found tumor size (along with pedicle destruction) to be the most important risk factor for vertebral body collapse in metastatically involved spines. Loading rate was found to have the

second strongest effect on metastatically involved vertebral body behavior. With inclusion of the poroelastic defect, increased loading rate resulted in more load carried by the fluid phase within the centrum, accounting for the increased pore pressures and lower axial compressive strains and displacements in the trabecular bone. Radial displacement along the transverse midline increased at higher loading rates, indicating escalating risk of potential neurologic compromise. These findings may indicate that the mechanism of burst fracture may differ in intact versus metastatically involved vertebral bodies. The presence of a defect which produces increased vertebral body pressurization and radial displacement may potentially allow a burst fracture pattern to occur without an endplate fracture. Variation of tumor tissue material properties did not have a large effect on the behavior of the trabecular bone centrum of the vertebral body, thus the primary site of the lytic tumor may not be of major significance in assessing failure risk.

While this study is limited by the use of a two-dimensional axisymmetric model, results of this simplified analysis provide a justification for the use of more complex three-dimensional poroelastic models and demonstrate the importance of loading rate. Due to the use of an idealized model, the results found here are used solely to make comparisons between the different cases (elastic/poroelastic, loading rate, tumor size, tumor tissue material properties). Although the cost of poroelastic modeling is relatively large, both in terms of determination of additional poroelastic material properties and extended computing time (especially for three-dimensional models), a purely elastic approach may not be sufficient to reproduce the complex behavior exhibited by this two phase structure.

Task 3: To incorporate poroelasticity and metastatic defects into a three-dimensional vertebral body model.

We have developed a poroelastic three-dimensional model of a spinal motion segment consisting of a vertebral body and adjoining intervertebral discs cut through the midsagital plane (Figure 7). The model includes the posterior arch but no other posterior elements. It has been designed to incorporate metastatic defects of varied size (encompassing 15%, 30% or 45% of the total trabecular volume, and with or without involvement of the pedicle) in order to allow the determination of the sensitivity to stress and posterior vertebral body fracture risk of varied configurations. No results have been obtained as of yet from analyses of the model.

CONCLUSIONS

Thus far, we are on track and meeting the schedule for the first 12 months provided in our initial proposal. While limited numbers of specimens have been tested at the present time, the experimental confined compression protocol developed appears to repeatably measure the poroelastic material parameters of tumor tissue specimens. These data are expected to correlate well with histologic findings in comparing tissue cellularity vs. hydraulic permeability and aggregate modulus. This information should prove useful not only to contribute to our further work in assessing burst fracture risk, but also in other areas of drug delivery and cancer treatment.

Our two-dimensional finite element model has demonstrated the need for utilizing poroelastic modeling techniques in analyzing spinal motion segments. Faster loading rates were shown to indicate an increased likelihood for endplate failure in intact vertebral bodies in concurrence with clinical observations. Increased tumor size was found to cause the greatest increase in metastatically involved vertebral body displacements, strains and pore pressure and suggested a greater risk for endplate and radial vertebral body failure as the size of defect increased. Higher loading rates applied to the metastatically involved models also indicated an escalating risk of a potential burst fracture pattern, whereas variation of tumor tissue material properties did not have a large effect in assessing failure risk. These simple models have formed a basis which has guided our work thus far in three-dimensional modeling and experimental validation with the goal of determining better criteria to assess burst fracture risk in patients with spinal metastases.

REFERENCES

1. Arguello, R. B. Baggs, R. E. Duerst, L. Johnstone, K McQueen, C. N. Frantz, 1990, "Pathogenesis of vertebral metastasis and epidural spinal cord compression," *Cancer*, 65: p. 98-106.
2. Berry, J. M. Moran, W. S. Berg and A. D. Steffee, 1987, "A morphometric study of human lumbar and selected thoracic vertebrae," *Spine*, 12(4): p. 362-367.
3. Constans, E. deDevitiis, R. Donzelli, R. Spaziante, J. F. Meder, C. Haye, 1983, "Spinal Metastases with Neurologic Manifestations Review of 600 Cases," *Journal of Neurosurgery*, 59: p. 111-118.
4. Carter and W. C. Hayes, 1977, "The compressive behavior of bones as a two-phase porous structure.," *J. Bone Joint Surg.*, 59A: p. 954-962.
5. Cheal, Hipp JA, Hayes WC, 1993, "Evaluation of finite element analysis for prediction of the strength reduction due to metastatic lesions in the femoral neck." *Journal of Biomechanics*, 26(3): p. 251-264.
6. Dimar, Voor M.J., Zhang Y.M., Glassman S.D., 1998, "A human cadaver model for determination of pathalogic fracture threshold resulting from tumorous destruction of the vertebral body.", *Spine*, 23(11): p. 1209-1214.
7. Downey, P. A. Simkin, and R. Taggart, 1987, "Compressive loading raises intraosseus pressure in the femoral head," *Trans ORS* 12: p. 496.
8. Fredrickson, Edwards W.T., Rauschning W., Bayley J.C., Yuan H.A., 1992, "Vertebral burst fractures: an experimental, morphologic, and radiographic study.", *Spine*, 17(9): p. 1012-1021.
9. Hill, Richards M.A., Gregory W.M., Smith P., Rubens R.D., 1993, "Spinal cord compression in breast cancer: a review of 70 cases.", British Journal of Cancer, 68(5): p. 969-973
10. Hipp, R. J. McBroom, E. J. Cheal, and W. C. Hayes, 1989, "Structural Consequences of Endosteal Metastatic Lesions in Long Bones," *J. of Orthopaedic Research,* 7: p. 828-837.
11. Holdsworth, 1970, "Fractures, dislocations, and fracture-dislocations of the spine," *J. Bone Joint Surg.[Am]*, 52(8):1534-1551.
12. Horst and P. Brinckmann, 1981, "Measurement of the Distribution of Axial Stress on the End-Plate of the Vertebral Body," *Spine*, 6(3): p. 217-232.
13. Houston, Rubens R.D., 1995, "The systemic treatment of bone metastases.", *Clinical Orthopaedics and Related Research*, (312): p. 95-104.
14. Keaveny, 1997, "Mechanistic approaches to analysis of trabecular bone.", *Forma*, 12: p. 267-275.
15. Keene, Sellinger D.S., McBeath A.A., Engber W.D., 1986, "Metastatic breast cancer in the femur. A search for the lesion at risk of fracture.", *Clinical Orthopaedics and Related Research*, (203): p. 282-288.
16. Lavaste, W. Skalli, S. Robin, R. Roy-Camille and C. Mazel, 1992, "Three-dimensional geometrical and mechanical modeling of the lumbar spine," *Journal of Biomechanics*, 25(10): p. 1153-1164.
17. McBroom, E. J. Cheal, and W. C. Hayes, 1988, "Strength Reductions From Metastatic Cortical Defects in Long Bones," *J. of Orthopaedic Research,* 6: p. 369-378.

18. McBroom, W. C. Hayes, W. T. Edwards, R. P. Goldberg and A. A. White, 1985, "Prediction of vertebral body compressive fracture using quantitative computed tomography," *Journal of Bone and Joint Surgery*, 67-A(8): p. 1206-1214.
19. McGowan, J. A. Hipp, T. Takeuchi, A. A. White III and W. C. Hayes, 1993, "Strength reductions from trabecular destruction within thoracic vertebrae," *J. Spinal Disord.*, 6(2): p. 130-136.
20. Mizrahi, M. Silva and W. C. Hayes, 1992, "Finite element stress analysis of simulated metastatic lesions in the lumbar vertebral body," *J Biomed Eng.*, November 14: p. 467-475.
21. Schultz, Andersson G., Ortengren R., Haderspeck K., Nachemson A., 1982, "Loads on the lumbar spine.", *Journal of Bone and Joint Surgery*, 5: p. 713-720.
22. Shimizu, Shikata J., Iida H., Iwasaki R., Yoshikawa J., Yamamuro T., 1992, "Posterior decompression and stabilization for multiple metastatic tumors of the spine." *Spine*, 17(11): p. 1400-1404.
23. Shirado, K. Kaneda, S. Tadano, H. Ishikawa, P. C. McAfee, K. E. Warden, 1992, "Influence of disc degeneration on mechanism of thoracolumbar burst fractures," *Spine*, 17: p. 286-292.
24. Silva, T. M. Keaveny and W. C. Hayes, 1996, "Load sharing between the shell and centrum in the lumbar vertebral body," *Spine, submitted*, .
25. Silva, Hipp J.A., McGowan D.P., Takeuchi T., Hayes W.C., 1993, "Strength reductions of thoracic vertebrae in the presence of transcortical osseus defects: effects of defect location, pedicle disruption, and defect size," *European Spine Journal*, 2: p. 118-125.
26. Sucher, Margulies J.Y., Floman Y., Robin G.C., 1994, "Prognostic factors in anterior decompression for metastatic cord compression. An analysis of results.", *European Spine Journal*, 3(2): p. 70-75.
27. Suwito, T. Keller, P. Basu, A. Weisberger, A. Strauss and D. Spengler, 1992, "Geometric and material property study of the human lumbar spine using the finite element method," *Journal of Spinal Disorders*, 5(Mar, 1): p. 50-59.
28. Toma, Venturino A., Sogno G., Formica C,. Bignotti B., Bonassi S., Palumbo R., 1993, "Metastatic bone tumors. Nonsurgical treatment. Outcome and survival.", *Clinical Orthopaedics and Related Research*, (295): p. 246-251.
29. Wong, V. L. Fornasier, and I. MacNab, 1990, "Spinal Metastases: The Obvious, the Occult, and the Impostors," *Spine*, 15(1): p. 1-3.
30. Yamashita, Koyama H., Inaji H., 1995, "Prognostic significance of bone metastases from breast cancer.", *Clinical Orthopaedics and Related Research*, (312): p. 89-94.

Table 1: Maximum Displacement (U) and Strain (E) Results in the Vertebral Body from the Elastic, Mixed Model and Poroelastic Analyses (@ 100 MPa/s).

	U1 (mm)	U2 (mm)	E11 ($x10^{-3}$)	E22 ($x10^{-3}$)	E33 ($x10^{-3}$)
Elastic	0.0493	-0.0477	3.56	-4.91	2.60
Mixed Free Flow	0.0479	-0.0733	3.58	-6.14	2.54
Mixed No Flow	0.0498	-0.0720	3.80	-6.06	2.64
Poroelastic	0.0561	-0.0674	3.78	-5.63	2.98

Table 2: Maximum Displacement (U) in the Vertebral Body and Pore Pressure (POR) Results in the Vertebral Body and Disc from the Poroelastic Model under Varied Loading Rates.

Loading Rate (MPa/s)	U1 (mm)	U2 (mm)	POR_{VB} (MPa)	POR_{DISC} (MPa)
10000	0.0488	-0.0672	0.294	1.80
1000	0.0507	-0.0673	0.302	1.80
100	0.0561	-0.0674	0.328	1.80
10	0.0670	-0.0627	0.497	1.80
4	0.0727	-0.0580	0.630	1.77

Table 3: Displacement (U, mm), strain (E), and pore pressure (POR, MPa) results in the vertebral trabecular bone of intact, 25% and 50% tumor volume models at loading rates of 10 and 100 MPa/s.

Loading Rate	Tumor Volume	U1	U2	E11*	E22*	E33*	POR
100 MPa/s	0 %	0.056	-0.067	0.378	-0.563	0.298	0.328
	25 %	0.142	-0.423	2.21	-1.35	2.21	0.832
	50 %	0.199	-0.975	3.08	-0.878	3.08	1.24
10 MPa/s	0 %	0.067	-0.063	0.443	-0.521	0.358	0.497
	25 %	0.139	-0.444	2.23	-1.43	2.23	0.768
	50 %	0.193	-1.10	3.50	-0.996	3.50	1.15

* $X10^{-2}$

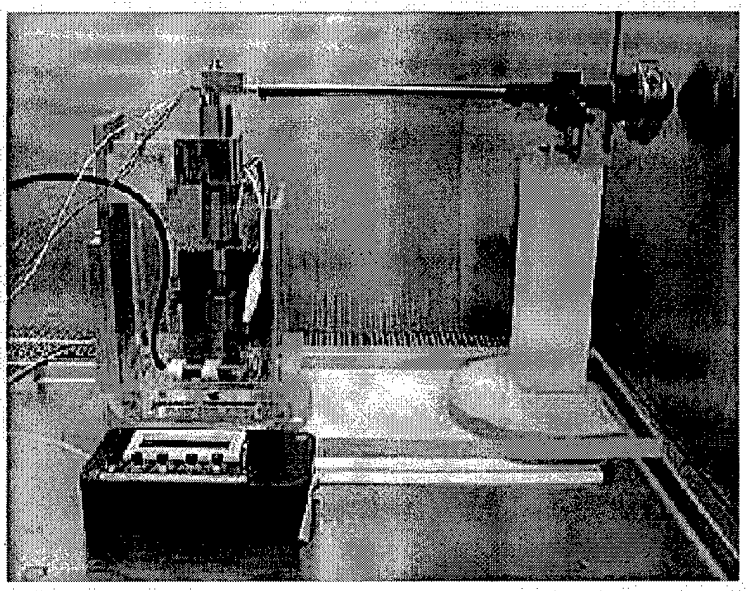

Figure 1: Confined compression experimental set-up

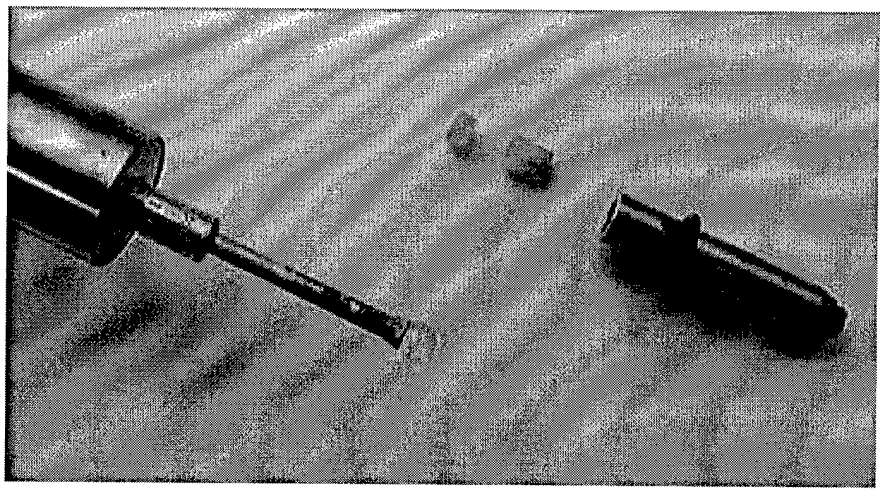

Figure 2: Confined compression chamber with glass porous platens, LVDT and plunger.

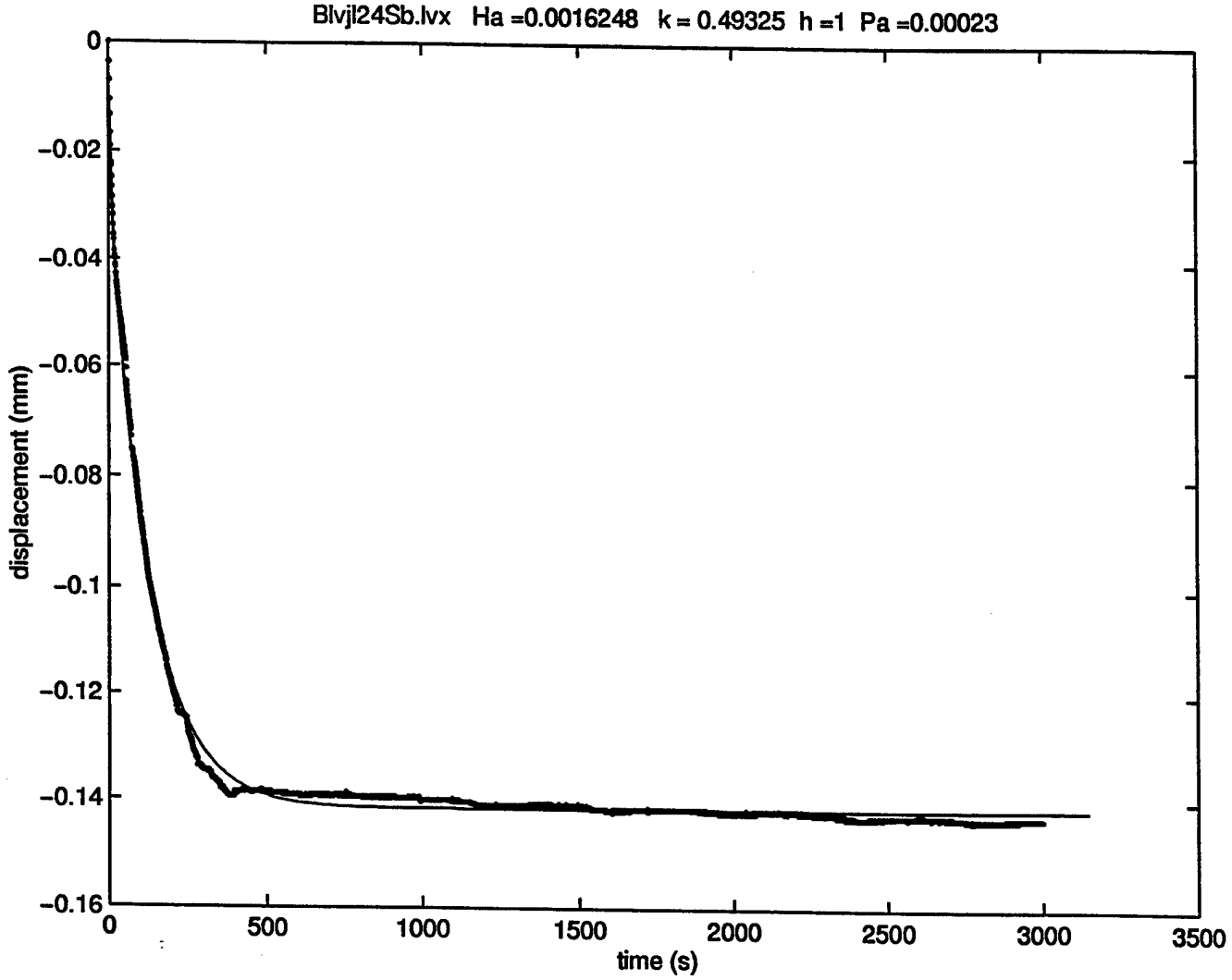

Figure 3: Experimental results and curve fit from confined compression testing on a specimen of breast tumor tissue which had metastasized to bone.

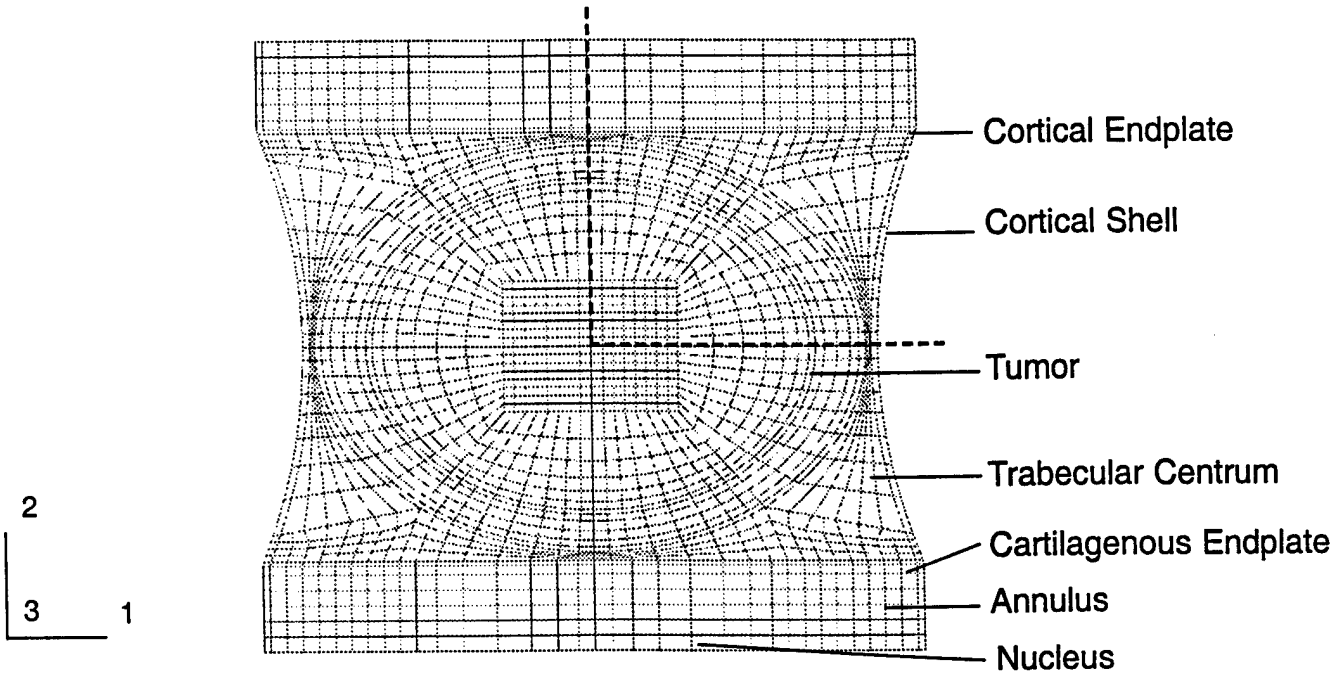

Figure 4: Finite element mesh of the spinal motion segment

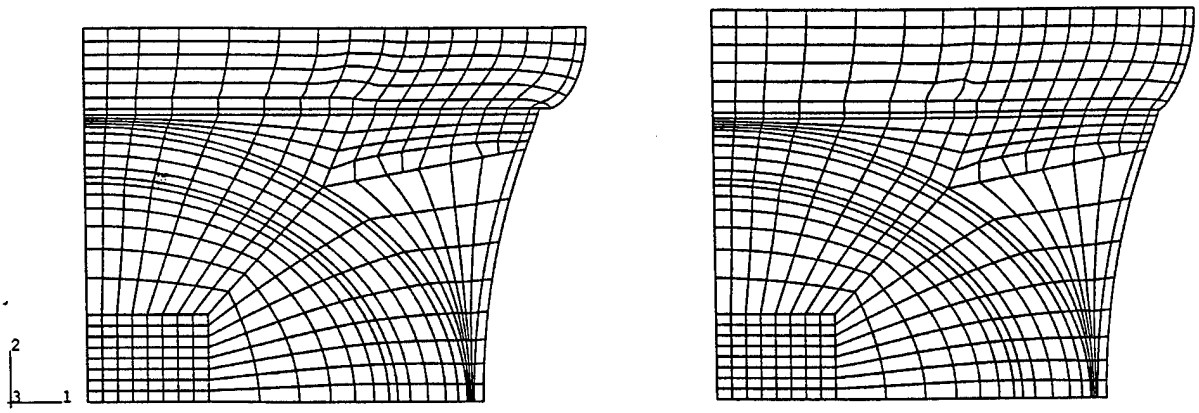

Figure 5: Deformed mesh of the fully elastic (left) and poroelastic (right) representations of the spinal motion segment under a 1MPa load.

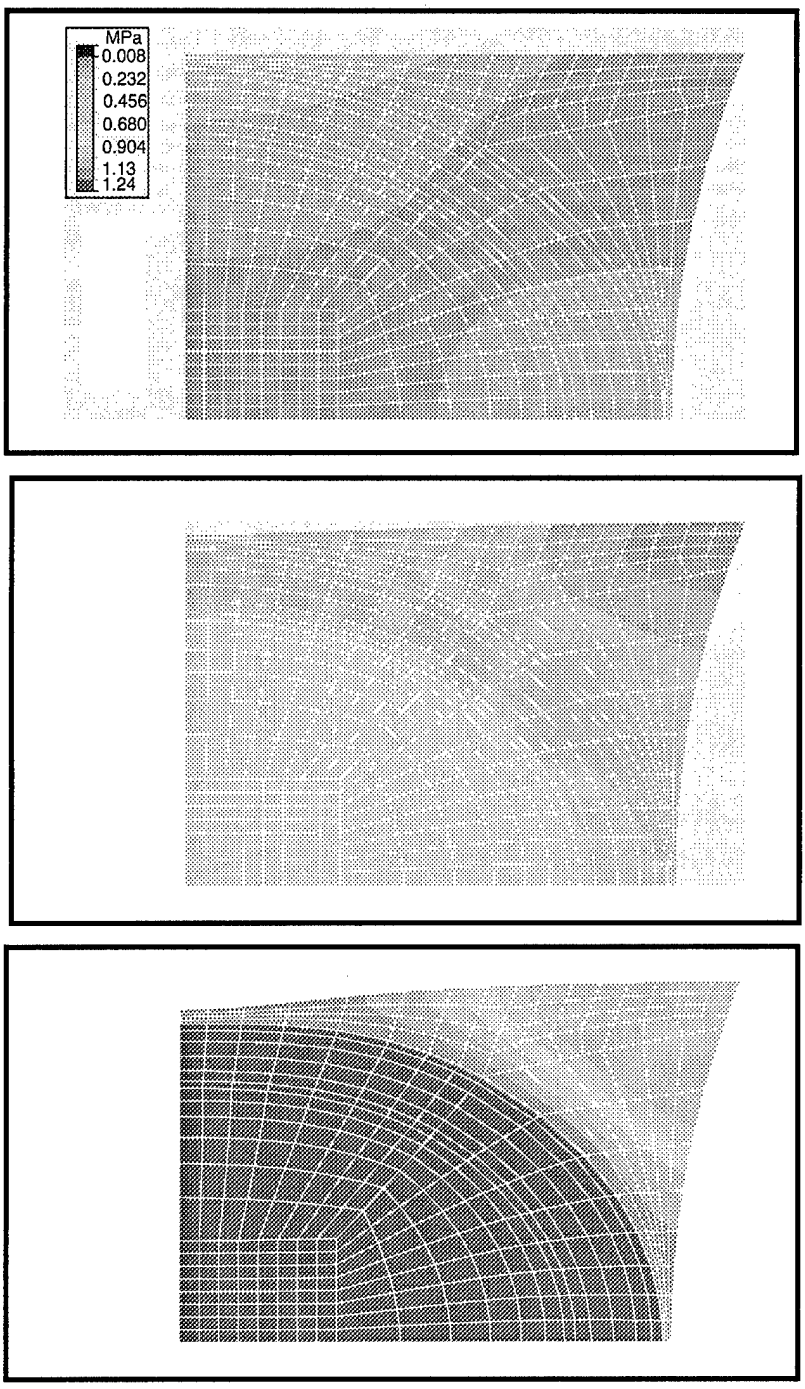

Figure 6 Pore pressure (POR) results developed in the vertebral trabecular bone of intact (top), 25% (mid) and 50% (bottom) tumor volume models under a 1 MPa load applied at a loading rate of 100 MPa/s.

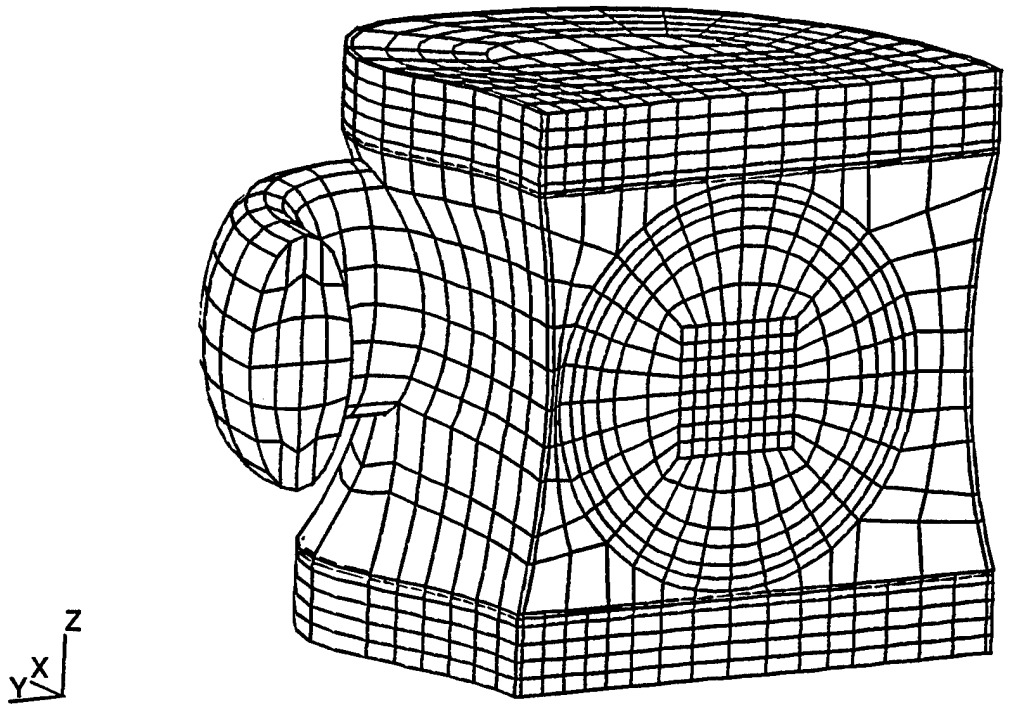

Figure 7: Three dimensional finite element mesh of a metastatically involved vertebral body and adjacent intervertebral discs.